

# 1 Microstructural Behaviors of Matrices Based on Polylactic Acid and 2 Polyhydroxyalkanoates

3 Juan Carlos Alzate Marin,<sup>†</sup> Sandra Rivero,<sup>\*,†,‡,§</sup> Adriana Pinotti,<sup>†,§</sup> Alejandro Caravelli,<sup>†</sup>  
 4 and Noemí Elisabet Zaritzky<sup>†,§</sup>

5 <sup>†</sup>Centro de Investigación y Desarrollo en Criotecnología de Alimentos (CIDCA), CONICET, Universidad Nacional de La Plata  
 6 (UNLP), Comisión de Investigaciones Científicas de la Provincia de Buenos Aires (CICPBA), 47 y 116 S/N, La Plata B1900AJJ,  
 7 Buenos Aires, Argentina

8 <sup>‡</sup>Facultad de Ciencias Exactas, Universidad Nacional de La Plata (UNLP), La Plata B1900AJJ, Buenos Aires, Argentina

9 <sup>§</sup>Facultad de Ingeniería, Universidad Nacional de La Plata (UNLP), La Plata B1900AJJ, Buenos Aires, Argentina

10 **ABSTRACT:** Individual films of polyhydroxyalkanoates (PHA) and polylactic acid (PLA) and their blends were developed by  
 11 solvent casting. PHA was obtained from activated sludges from a wastewater-treatment system at a laboratory scale. This work  
 12 focused on analyzing the microstructural properties and thermal behaviors of individual films of PHA and PLA as well as those  
 13 of their blends. The behaviors of the biodegradation processes of the individual films and blends were examined from a  
 14 microstructural point of view. ATR-FTIR spectra indicated the existence of weak molecular interactions between the polymers.  
 15 The formulation of blend films improved the crystallinity of PLA; additionally, it induced the polymer-recrystallization  
 16 phenomenon, because crystallized PHA acted as a PLA-nucleating agent. This phenomenon explains the improvements in the  
 17 films' water-vapor-barrier properties. The blends exposed to a biodegradation process showed an intermediate behavior between  
 18 PLA and PHA, leading to a consistent basis for designing systems tailored to a particular purpose.

19 **KEYWORDS:** *biopolymers, polymer blends, infrared spectroscopy, crystallinity, modulated DSC, morphology*

## 20 ■ INTRODUCTION

21 Polyhydroxyalkanoate (PHA) is a family of biopolyesters  
 22 synthesized by microorganisms from various carbon sources;  
 23 they are accumulated intracellularly under nutrient stress and  
 24 act as carbon and energy reserves.<sup>1</sup> PHAs can be produced by  
 25 both pure and mixed microbial cultures. Mixed cultures have  
 26 the advantage that they do not need sterile conditions and are  
 27 better able to adapt to complex substrates, such as industrial  
 28 wastes, than pure cultures.<sup>2</sup> For this, wastes from the dairy  
 29 industry, the sugar industry, forestry, and biodiesel production  
 30 can be utilized.<sup>3</sup> Cheese whey is a surplus material from the  
 31 dairy industry that is mainly discharged to both soils and water  
 32 bodies, causing serious environmental problems. PHA  
 33 production from cheese whey could revalorize this dairy  
 34 subproduct and, at the same time, solve the waste-disposal  
 35 problems.

36 A relevant characteristic of PHA is its versatility, because  
 37 there are more than a hundred different monomers, including  
 38 hydroxyvalerate and butyrate among others. The properties of  
 39 the synthesized polymer are modified depending on the  
 40 position of its functional groups and degrees of polymerization.  
 41 This chemistry allows PHAs to be tailored to provide similar  
 42 properties to traditional thermoplastics, such as polyethylene  
 43 (PE) and polypropylene (PP), while maintaining biodegrad-  
 44 ability.<sup>4</sup>

45 Polylactic acid (PLA), a thermoplastic aliphatic polyester  
 46 derived from lactic acid (2-hydroxy propionic acid), can be  
 47 produced by condensation and polymerization directly from its  
 48 basic building block, lactic acid, which is derived from the  
 49 fermentation of sugars from carbohydrates sources, such as

corn starch; cassava root, chips, and starch; and sugar cane.<sup>5</sup> 50  
 Polylactic acid is produced at the largest industrial scale of all 51  
 biodegradable polymers, and it is considered the most 52  
 promising candidate for replacing conventional plastics.<sup>6</sup> It is 53  
 being used in biomedical applications, for bottle production, 54  
 for filament production in 3D printing, and for compostable- 55  
 food-packaging production. It is also being evaluated as a 56  
 material for tissue engineering. Mass production has reduced 57  
 the cost of PLA production, making it an economically viable 58  
 choice for the fabrication of containers, plastic bags, and fibers. 59  
 Commercial-scale plants today produce hundreds of thousands 60  
 of tons of PLA per year.<sup>7</sup> 61

By controlling the molecular architecture, suppliers are able 62  
 to tailor the polymer to specific applications. Consequently, 63  
 new and improved grades of bioplastic resins are constantly 64  
 being introduced to the market. NatureWorks LLC focuses on 65  
 a multistep procedure involving the condensation reaction of 66  
 aqueous lactic acid for the production of a low-molecular- 67  
 weight PLA prepolymer. It is converted into a blend of lactide 68  
 stereoisomers in order to produce a large spectrum of PLA 69  
 grades.<sup>8</sup> The films based on PLA have excellent optics and 70  
 good machinability, barrier, and mechanical properties.<sup>5</sup> 71

PLA and PHA polymers are polyesters and are used in 72  
 consumer products by a wide industrial sector as a result of 73  
 their biocompatibility and sustainability.<sup>9</sup> They have thermal 74

**Received:** March 25, 2018

**Revised:** July 14, 2018

**Accepted:** July 23, 2018

**Published:** July 23, 2018

75 behaviors comparable to those of some conventional polymers,  
76 and this has generated much interest in exploring their physical  
77 and structural properties to identify potential applications.<sup>10</sup>

78 The combination of the two polymers allows the design of  
79 new materials with tailorable properties differing meaningfully  
80 from those of each component by adjusting the advantages of  
81 each polymer in order to obtain materials for different  
82 applications. In this sense, the formulation of blend systems  
83 is easier and faster than copolymerization methods.<sup>11</sup> There  
84 are many studies focused on PLA modification, such as the  
85 addition of modifiers and copolymerization.<sup>12</sup> The addition of  
86 a highly ordered stereochemical structure, such as that of PHA,  
87 could improve the film properties of PLA.<sup>13,14</sup> In this sense,  
88 blending PLA with another biobased and biodegradable  
89 material, PHA, in order to obtain tailor-made materials  
90 constitutes a promising alternative.

91 This work focused on analyzing the microstructural  
92 properties and thermal behaviors of PHA and PLA individual  
93 films as well as those of their blends. Furthermore, the  
94 biodegradation processes of the individual films and PLA/PHA  
95 blends were examined from a microstructural point of view.

## 96 ■ MATERIALS AND METHODS

97 Polylactic acid (PLA), grade 4043D in pellet form (98% L-lactide with  
98 a D-isomer content of approximately 2%) and designed for the  
99 production of films, was purchased from Natureworks under the  
100 trademark Ingeo. As is well-known, the production of PLA involves  
101 the conversion of starch in dextrose via a hydrolysis process and  
102 fermentation by microorganisms to synthesize the chain of the  
103 polylactide polymer.

104 Polyhydroxyalkanoate (PHA) was obtained from activated sludges  
105 from a wastewater-treatment system at the laboratory scale (CIDCA).  
106 A two-stage biological system was proposed to produce PHA by  
107 aerobic mixed culture from hydrolyzed cheese whey. The first step  
108 involved the selection of PHA-accumulating organisms using an  
109 aerobic sequencing batch reactor (SBR) operated under a feast–  
110 famine regime. Then, there was the stage of PHA accumulation in an  
111 aerobic batch reactor that was inoculated with biomass taken from  
112 SBR enriched with PHA-accumulating bacteria.

113 **Extraction and Quantification of PHA.** Extraction and  
114 characterization of PHA from the batch-reactor biomass were  
115 performed following the method proposed by Venkateswar Reddy  
116 et al.<sup>15</sup> A hydroxybutyrate–hydroxyvalerate (HB–HV) copolymer  
117 with a purity of 96% and a molar relation 95:5 HB–HV was obtained.

118 **Film Preparation.** The films were prepared by dissolving PHA  
119 and PLA in chloroform at 1 and 2% (w/v), respectively, under stirring  
120 for 3 h. PLA/PHA mixtures were prepared in the following  
121 proportions: 20/80, 40/60, 60/40, and 80/20 (w/w). They were  
122 stirred for 30 min at 60 °C.

123 Filmogenic solutions of PLA, PHA, and their blends were cast into  
124 glass Petri dishes (9 cm diameter) that were left under a fume hood.  
125 Later, the samples were dried in a vacuum oven at 60 °C to ensure  
126 solvent removal from the matrices. When the solutions were cast,  
127 constant mass–molding-area ratios were maintained in order to  
128 ensure uniform thicknesses in the different samples, because the  
129 control solutions (PLA and PHA) had different concentrations.

130 Film thickness was measured by means of a coating-thickness gauge  
131 (Check Line DCN-900) for nonconductive materials on nonferrous  
132 substrates. For each specimen, at least 14 measurements at different  
133 positions were taken.

134 **Water-Vapor Permeability.** Water-vapor-permeability (WVP)  
135 tests were carried out according to the technique described by Rivero  
136 et al.<sup>16</sup> based on a modified version of ASTM<sup>17</sup> method E96. A  
137 permeation cell maintained at 20 °C was used for the assays. Eight  
138 measurements were performed once steady-state conditions were  
139 reached. All measurements were performed at least four times for each  
140 specimen.

**Thermal Analysis by MDSC.** Thermal analysis of the samples  
141 was conducted by the modulated-differential-scanning-calorimetry  
142 (MDSC) technique. Q100 (TA Instruments) controlled by a TA  
143 5000 module (TA Instruments) and equipped with a cryogenic-  
144 quench-cooling accessory was used under a N<sub>2</sub> atmosphere. This  
145 technique allowed us to measure the calorific capacity of the sample  
146 and simultaneously differentiate between the reversible (dependent  
147 on the calorific capacity) and irreversible events (dependent on the  
148 time and temperature) that the sample experienced. Likewise, it  
149 allowed the resolution of complex transitions.

150 A standard heating ramp of 10 °C min<sup>-1</sup> with a modulation-  
151 temperature amplitude of 0.5 °C and a modulation period of 60 s was  
152 used. The first scan (heating) was performed in order to delete the  
153 thermal story from –50 °C up to 200 °C. Once the first scan was  
154 completed, the sample was cooled to –80 °C, and then a second  
155 heating scan was recorded. Informed results were the averages of two  
156 replicates to ensure reproducibility of the results.

157 The results were analyzed by using the Universal Analysis V1.7F  
158 software (TA Instruments). Different parameters were determined  
159 from the obtained thermograms: melting temperature ( $T_m$ ), enthalpy  
160 corresponding to the area of the endothermic peak ( $\Delta H_m$ ),  
161 crystallization temperature during the cooling stage ( $T_c$ ), crystal-  
162 lization enthalpy ( $\Delta H_c$ ), and glass-transition temperature ( $T_g$ )  
163 determined from the reversible signal.

164 **ATR-FTIR Spectroscopy.** The interactions between the system  
165 components were analyzed using the ATR-FTIR technique. Spectra of  
166 the samples were registered by using the Thermo Scientific Nicolet  
167 iS10 FT-IR Spectrometer in the wavenumber region of 4000–400  
168 cm<sup>-1</sup>, performing 64 scans at a 4 cm<sup>-1</sup> resolution. Specimens were  
169 placed onto the diamond ATR crystal (Smart iTX accessory), and the  
170 software Omnic 8 (Thermo Scientific) was used for the data-analysis  
171 process. To ensure the reproducibility of the results, the tests were  
172 performed in triplicate.

173 **X-ray Diffraction.** X-ray diffractograms of individual PVA and  
174 PLA films and their blends were evaluated by using an X'Pert Pro P  
175 Analytical Model PW 3040/60 (Almelo) operated at room temper-  
176 ature. The Cu K $\alpha$  radiation (1.542 Å) was generated at 30 mA and 40  
177 kV. Scattered radiation was detected in an angular range of 3–60°  
178 (2 $\theta$ ) at a step size of 0.02°. The crystallinity degree (CD) was  
179 calculated following the procedure described in previous works.<sup>18,19</sup>

180 **Structural Studies by SEM.** The microstructures of the matrices  
181 were examined by using an FEI model Quanta 200 scanning electron  
182 microscope. Individual films and blend matrices were immersed in  
183 liquid nitrogen and fractured cryogenically. Samples were mounted  
184 onto metal stubs by using double-sided tape and observed at low  
185 pressure and an acceleration voltage of 12.5 kV, without any metal or  
186 carbon coating.

187 **Biodegradation Test.** A series of plastic pots (400 cm<sup>3</sup>) were  
188 used as soil containers, and the microflora present was used as a  
189 degrading medium. Square specimens of 3 × 3 cm with a thickness of  
190 approximately 25  $\mu$ m on average were put into a plastic mesh to allow  
191 the access of moisture and microorganisms and the retrieval of  
192 degraded specimens. In order to guarantee aerobic degradation, the  
193 film samples were buried. The samples were conditioned at a relative  
194 humidity of 50% and a temperature of 20 °C. Containers were  
195 sprayed regularly with a defined and constant amount of water.  
196 Similar conditions were employed by Rivero et al.<sup>20</sup> At specific time  
197 intervals, specimens were recovered from the soil and cleaned with a  
198 brush to avoid any possible damage of the structure.

199 In accordance with the described methodology in ASTM D5988-  
200 03,<sup>21</sup> a ratio of 1 g of compost per 25 g of soil was used. Studies of the  
201 morphology of the degraded films were performed by means of SEM,  
202 MDSC, and ATR-FTIR analysis.

203 **Statistical Analysis.** For statistical analysis, version 10.0 of Systat-  
204 software (Systat, Inc.) was used. Analysis of variance (ANOVA),  
205 linear regressions, and Fisher's least-significant-difference test for  
206 mean comparison were performed. The significance level used was  
207 0.05.

## 209 ■ RESULTS AND DISCUSSION

210 **Thermal Analysis.** The thermograms obtained by means  
 211 of MDSC from PLA, PHA, and their blends can be observed in  
 212 **Figure 1**, where the stages of heating and cooling are shown.  
 213 The temperatures of the thermal transitions and the enthalpy  
 214 values ( $\text{J g}^{-1}$ ) of the characteristic events during the heating

and cooling stages obtained from MDSC curves are 215 t1  
 summarized in **Table 1**. 216 t1

As it is possible to see in **Figure 1a**, the thermal analysis 217  
 allowed us to observe a peak for each individual film, 218  
 attributable to the melting of the crystalline domains 219  
 corresponding to PLA and PHA at 147.7 and 172.7 °C, with 220  
 the associated enthalpies of 20.1 and 86.6  $\text{J g}^{-1}$ , respectively. 221  
 The intensity of the melting peak is related to the number of 222  
 crystals or crystalline populations (crystalline fraction) that 223  
 exist in the material when the melting occurs. Using MDSC, 224  
 Thellen et al.<sup>4</sup> reported that crystal melting is produced at 225  
 higher temperatures in samples of PHA containing lower 226  
 percentages of valerate, because as the valerate content 227  
 increases, the onset of crystal melting occurs at lower 228  
 temperatures. In the present study, the PHA thermograms 229  
 evidenced the presence of a peak with a shoulder, which could 230  
 represent the melting of crystal lamellae, as was reported by 231  
 Thellen et al.<sup>4</sup> for extruded PHA. 232

On the other hand, PHA films exhibited a  $T_g$  at  $-4.7$  °C, 233  
 whereas PLA showed a marked transition at 58.1 °C (**Figure** 234  
**1c**). Glass-transition temperatures ranging from 2.7 to  $-4.4$  °C 235  
 for a PHA matrix obtained by casting were reported by da Silva 236  
 et al.<sup>22</sup> 237

The thermograms of all the mixtures exhibited PLA- 238  
 recrystallization peaks at 107 °C; this transition was more 239  
 evident with higher PLA proportions in the mixture (**Figure** 240  
**1a**). These results indicate that the incorporation of PHA 241  
 contributes to the process of recrystallization of PLA in all the 242  
 blend formulations. This effect was more marked in the 80/20 243  
 blend, a behavior that could be explained by bearing in mind 244  
 that a low proportion of crystalline domains of PHA dispersed 245  
 in a continuous matrix of PLA induced the phenomenon of 246  
 nucleation of this latter polymer. The presence of double 247  
 melting temperatures in the PLA/PHA blends corresponds to 248  
 the melting of both the “as formed” and recrystallized 249  
 polymer.<sup>10</sup> 250

According to Abdelwahab et al.<sup>10</sup> and Ikehara et al.,<sup>23</sup> 251  
 recrystallization strongly depends on the melting-temperature 252  
 differences among the components of the mixture. When the 253  
 $T_m$  difference is very large, the component with the higher 254  
 melting temperature crystallizes first, and its spherulites 255  
 contribute to fill all the volume. 256

The 20/80 blend exhibited a peak at 171.9 °C because of the 257  
 melting of the PHA crystalline fraction and a shoulder at 148.4 258  
 °C corresponding to the melting of PLA. The 80/20, 60/40, 259  
 and 40/60 blends exhibited two endothermic transitions; the 260  
 enthalpy associated with the first event diminished with the 261  
 incorporation of a higher proportion of PHA to the blend, 262  
 whereas the enthalpy of the endothermic peak, characteristic 263  
 of the PHA-crystalline phase, became more prominent (**Figure 1a** 264  
 and **Table 1**). These findings were in accordance with a higher 265  
 crystalline degree. 266

From the obtained DSC curves, two  $T_g$  values were observed 267  
 irrespective of the blend composition. These results suggest 268  
 that the analyzed PLA/PHA blends are immiscible in the 269  
 amorphous state (**Figure 1c**). 270

According to Lipatov and Alekseeva,<sup>24</sup> the appearance of 271  
 two transitions associated with the glass-transition temper- 272  
 atures supports the existence of a partially miscible system (i.e., 273  
 materials with a heterogeneous biphasic structure). 274

During the cooling step, PHA exhibited a peak of 275  
 crystallization at 58.7 °C with an associated enthalpy of 48.4 276  
 $\text{J g}^{-1}$ , whereas the thermogram of PLA did not show this 277

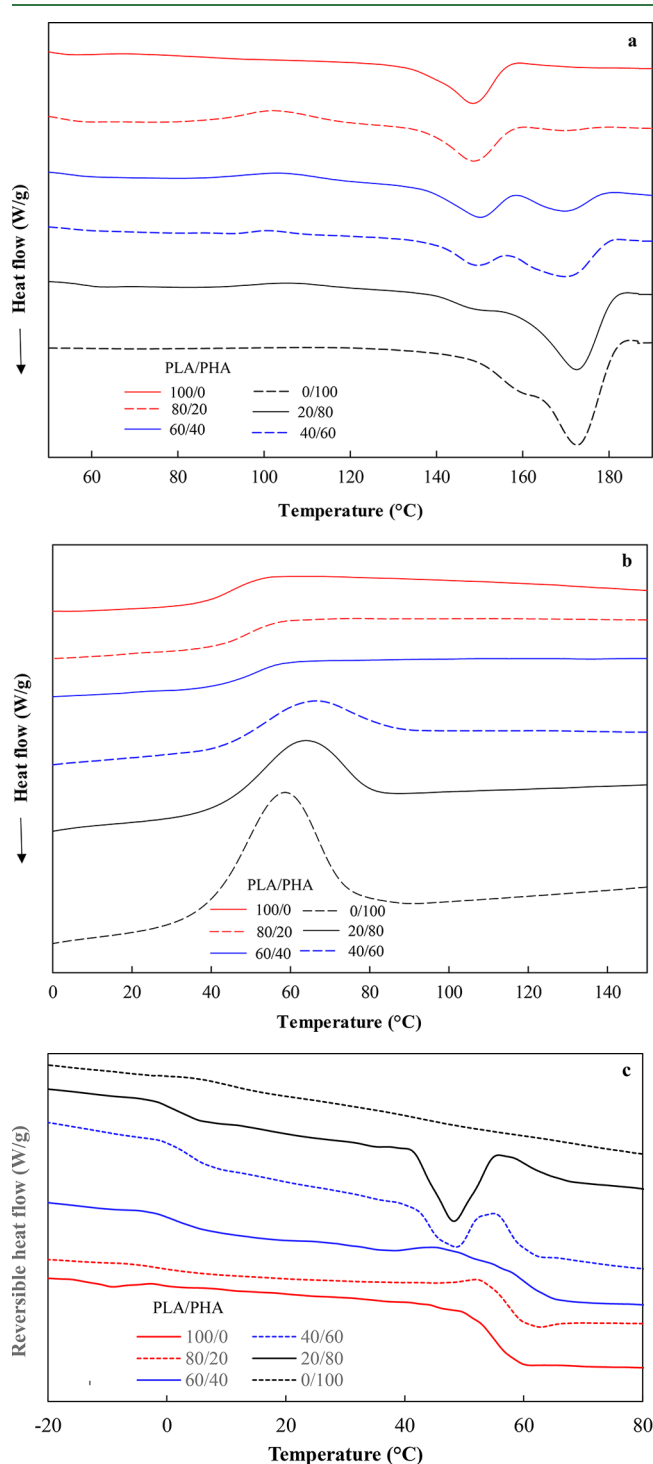


**Figure 1.** MDSC curves of individual (PLA and PHA) and blend films with different proportions of PLA/PHA showing (a) heating stage, (b) cooling stage, and (c) reversing heat flow ( $\text{W g}^{-1}$ ), evidencing the glass-transition temperatures ( $T_g$ ) of each component.

Table 1. Thermal Analysis of Single and Blend Matrices with Different Proportions of PLA/PHA<sup>a</sup>

PLA/PHA	heating stage				cooling stage	
	characteristic events of PHA		characteristic events of PLA		characteristic events of PHA	
	$T_m$ (°C)	$\Delta H_m$ (J g <sup>-1</sup> )	$T_m$ (°C)	$\Delta H_m$ (J g <sup>-1</sup> )	$T_c$ (°C)	$\Delta H_c$ (J g <sup>-1</sup> )
100/0	—	—	147.7(1.0) a	20.1(1.3) c	—	—
80/20	170.4(1.2) a	1.5(0.07) a	150.3(1.9) a	20.0(0.7) c	—	—
60/40	169.9(0.6) a	9.1(0.1) b	149.8(0.6) a	13.4(0.5) b	—	—
40/60	170.3(0.4) a	18.8(0.7) c	149.5(0.9) a	5.8(0.1) a	65.6(0.5) b	18.8(0.1) a
20/80	171.9(0.8) a	61.7(1.2) d	—	—	65.9(3.8) b	31.4(1.9) b
0/100	172.7(0.1) a	86.6(0.1) e	—	—	58.8(0.5) a	48.4(0.4) c

<sup>a</sup>Different letters in the same column indicate significant differences ( $p < 0.05$ ) among samples.

278 transition (Figure 1b and Table 1). Taking these results into  
279 account, it is possible to infer that the crystallinity of PHA is  
280 greater than that of PLA.

281 The thermal analysis of the PLA/PHA mixtures showed that  
282 the peak of crystallization attributable to PHA was observed  
283 only in the 20/80 and 40/60 mixtures, with a minor associated  
284 enthalpy regarding a single PHA matrix (Figure 1b). On the  
285 other hand, the thermograms of the individual PLA film and  
286 the 60/40 and 80/20 mixtures did not exhibit this thermal  
287 transition (Figure 1b). Nevertheless, an event was observed at  
288 57.7 °C attributable to the glass-transition temperature of the  
289 PLA-enriched phase. Similar results were informed by Arrieta  
290 et al.,<sup>12</sup> Furukawa et al.,<sup>25</sup> and Zhang and Thomas,<sup>11</sup> indicating  
291 that these results are a signal of the fact that the PHA in the  
292 mixtures does not crystallize during the cooling stage when it is  
293 the minor proportion.

294 **Microstructural Analysis. FTIR Analysis.** From the ATR-  
295 FTIR spectra, the functional characteristic groups of PLA and  
296 PHA were identified (Figure 2a,b). They are consistent with  
297 those reported in the literature.<sup>5,26,27</sup>

298 In the PLA spectrum, the band located at 1746 cm<sup>-1</sup> is a  
299 strong peak that corresponds to the stretching of the carbonyls'  
300 amorphous phase.<sup>5</sup> The bands located at 1180 and 1080 cm<sup>-1</sup>  
301 belong to the asymmetric and symmetric stretching vibrations  
302 of C—O—C. As is known, PLA is a hydrophobic polymer  
303 because of the presence of —CH side groups. The peaks at  
304 about 2997 and 2946 cm<sup>-1</sup> correspond to the asymmetric and  
305 symmetric stretching vibrations of the —CH groups in the side  
306 chains, respectively (data not shown).

307 On the other hand, in the PHA spectrum, the peak at 1719  
308 cm<sup>-1</sup> is attributable to the stretching of the crystalline carbonyl  
309 group, and the stretching of the carbonyl group of the  
310 amorphous phase is virtually imperceptible. The 40/60 and  
311 20/80 samples exhibited peaks at 1748 and 1755 cm<sup>-1</sup> (Figure  
312 2b), which were assigned to the amorphous and crystalline  
313 bands of PLA, respectively.<sup>24</sup>

314 Furthermore, Figure 2a,b depicts the ATR-FTIR spectra of  
315 the PLA/PHA blend matrices. The spectra of the 80/20 and  
316 60/40 compositions followed a similar pattern to that of the  
317 pristine PLA, whereas the 40/60 and 20/80 mixtures were  
318 identified mainly with the PHA spectrum. All of them unfolded  
319 both bands corresponding to the stretching of carbonyls  
320 located at 1746 and 1719 cm<sup>-1</sup> due to PLA and PHA phase,  
321 respectively (Figure 2a,b).

322 In the cases of the 80/20, 60/40, and 40/60 blends, the  
323 bands in the C—O—C and C—C stretching and CH  
324 deformation mode region (1300–1000 cm<sup>-1</sup>) are visualized  
325 at about the same wavenumbers as those of pure PHA (Figure  
326 2a,b).

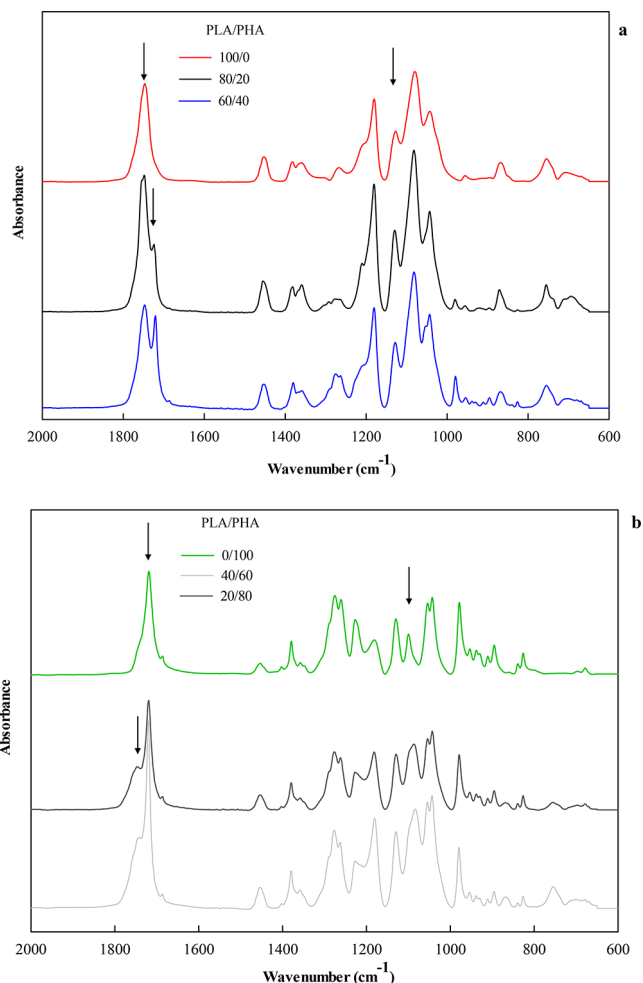
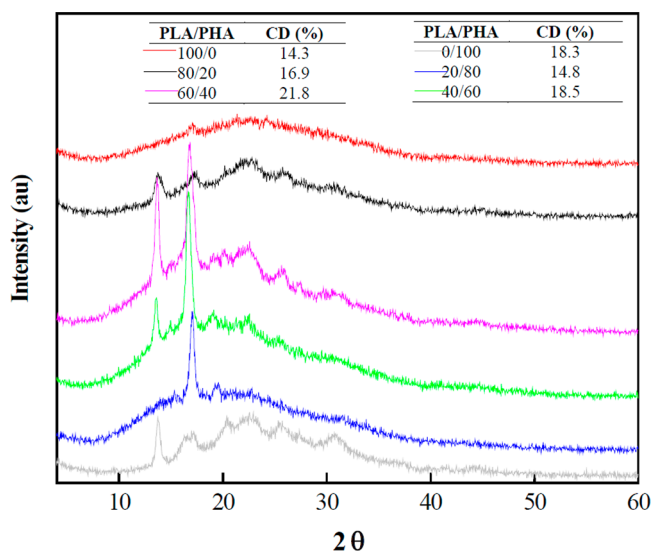


Figure 2. ATR-FTIR spectra of individual (PLA and PHA) and blend matrices with different proportions of PLA/PHA.

It is noteworthy that the intensities of these bands were  
interdependent and mutually dependent, one being increased  
at the expense of the other, meaning that the ratio of intensities  
of these two bands changed in agreement with the ratio of the  
individual components. These results allowed us to infer the  
immiscibility of these components and that there were no  
strong molecular interactions between the polymers.

**X-ray Diffraction.** The typical diffraction patterns of  
individual PHA and PLA and those of the composite films  
are depicted in Figure 3. The X-ray diffractogram of the PLA  
films exhibited a pattern corresponding to an amorphous  
material with a peak located at  $2\theta = 17^\circ$ , which was associated  
with the reflection of the crystals of the polymer;



**Figure 3.** X-ray diffractograms of individual (PLA and PHA) and blend films with different proportions of PLA/PHA. Table inset shows the crystallinity degrees (%) of the samples.

340 estimated crystallinity degree was 14.3% (table insert in Figure  
341 3). In contrast, PHA is a highly ordered polymer, and it is  
342 known to crystallize in an orthorhombic cell.<sup>10</sup>  
343 X-ray-diffraction analysis was used to determine the  
344 crystalline structures and crystallinity degrees of the blends.  
345 The PHA spectrum showed diffraction peaks at  $2\theta = 13.8$  and  
346  $17^\circ$ , corresponding to the (020) and (110) planes,  
347 respectively.<sup>11</sup> Additionally, reflections at  $2\theta = 20.3, 22.4,$

25.4, and  $30.8^\circ$  were detected, which were characteristics of  
the PHA polymer, its CD being 18.3%.<sup>14</sup>

The inclusion of PHA in the blends increased the  
crystallinity of the materials. The highest crystallinity degrees  
of the 60/40 and 40/60 blends were confirmed by means of X-  
rays (table insert in Figure 3). The diffractograms showed  
peaks of higher intensity in relation to individual matrices.

This behavior allows us to infer that PHA induces the  
recrystallization of PLA due to its capacity to act as an agent of  
nucleation. According to Furukawa et al.<sup>24</sup> and Zhang and  
Thomas,<sup>11</sup> it generates better packing density of the polymeric  
segments and promotes better adhesion and interaction at the  
interface level. However, the microstructure, porosity, and  
permeability of the matrix seem to depend on the PLA/PHA  
proportions, as presented below.

**SEM Observations.** From the macroscopic point of view,  
the blend of the two polymers appeared to be well mixed in the  
matrices with no apparent phase separation, although FTIR  
showed the immiscibility of both components. The average  
thickness of the films was  $25 \mu\text{m}$ , which was corroborated by  
microscopic analysis. As it can be seen in Figure 4, all matrices  
presented homogeneous appearances irrespective of the PLA/  
PHA ratio.

The films showed important differences when analyzed in  
the cross-sections of single or blend matrices. PLA-only films  
showed a homogeneous appearance, without pores and with  
good structural integrity. Addition of the PHA polymer led to  
films whose cross-section was rough, giving a structure with a  
fibrous appearance (Figure 4).

The cross-sections and surfaces of the 20/80 and 40/60  
mixtures revealed the presence of an orderly structure,  
attributable to the growth and crystallization of the spherulites

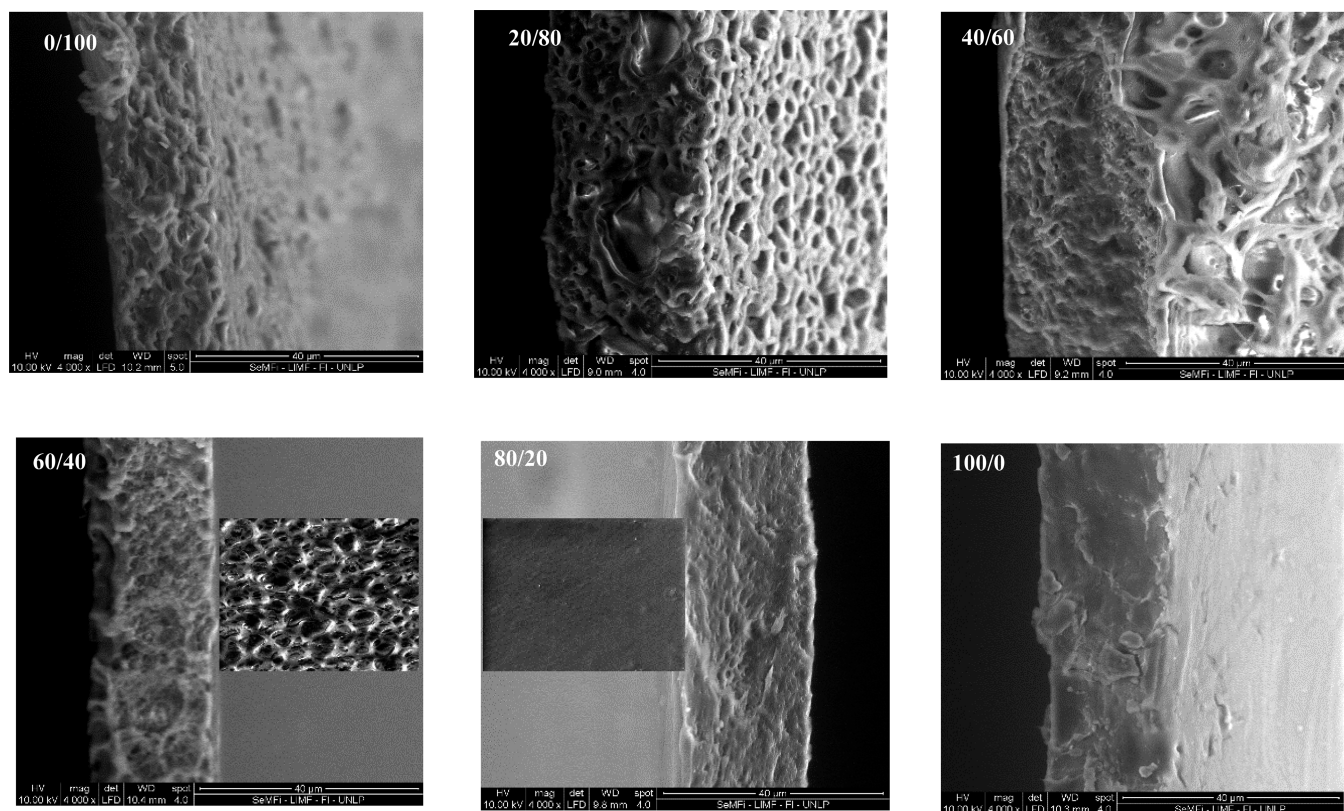


**Figure 4.** Cross-section SEM micrographs of individual (PLA and PHA) and blend films with different proportions of PLA/PHA.

380 of PHA, proving to be a network formed by codomains  
381 corresponding to the different polymers with a granular,  
382 interspersed appearance and a repetitive pattern. It is  
383 important to remark that the highest proportion of PHA in  
384 the blends (PLA/PHA = 20/80) evidenced a porous  
385 microstructure as a result of the structural arrangement  
386 between the polymers. According to Abdelwahab et al.,<sup>10</sup> the  
387 interface interactions between the PHA and PLA phases could  
388 influence the nucleation phenomenon as supported by the  
389 XRD results.

390 These micrographs reinforced the results of immiscibility  
391 obtained by other techniques. As the PLA proportion  
392 increased, the morphology of the matrices became more  
393 homogeneous and less rough, until the 80/20 mixture  
394 presented an appearance where the PLA-enriched phase  
395 formed a continuous domain in which the PHA-enriched  
396 phase was dispersed and homogeneously distributed, as can be  
397 seen in Figure 4.

398 **Water-Vapor Permeability.** Table 2 shows the WVP values  
399 of the individual films and PLA/PHA blends. The formulation

**Table 2. Water-Vapor-Barrier Properties of the Individual (PLA and PHA) and Blend Films with Different Proportions of PLA/PHA<sup>a</sup>**

PLA/PHA	WVP ( $\times 10^{11}$ g s <sup>-1</sup> m <sup>-1</sup> Pa <sup>-1</sup> )
100/0	1.73(0.25) b
80/20	0.62(0.06) a
60/40	0.68(0.07) a
40/60	0.72(0.05) a
20/80	2.22(0.38) b
0/100	2.24(0.30) b

<sup>a</sup>Different letters indicate significant differences ( $p < 0.05$ ) among samples.

400 of the blend matrices improved the barrier properties of the  
401 materials, obtaining a reduction of 40% in the WVP values for  
402 the 40/60, 60/40, and 80/20 blends compared with the values  
403 of the individual films (Table 2). Meanwhile, the 20/80 blend  
404 did not show significant differences ( $p > 0.05$ ).

405 According to Arrieta et al.,<sup>12</sup> the crystallization of PLA  
406 reduces the water-vapor permeability because the crystals  
407 decrease the volume of the amorphous phase, generating a  
408 path of greater tortuosity and reducing mass matter transfer.

409 The improvement of the barrier properties is related to the  
410 higher crystallinity of the PLA/PHA blend matrices, as  
411 observed by the X-ray diffraction technique and the MDSC  
412 thermal analysis.

413 **Soil-Biodegradation Studies.** The influence of the micro-  
414 structure developed during the formulation of the blends on  
415 the biodegradation process was examined. A morphological  
416 study by SEM during soil-biodegradation experiments was  
417 complementary to visual examination as it helped to confirm  
418 the existence of structural modifications in the films, allowing a  
419 detailed evaluation of the degradation process.

420 The results showed that the degradation behavior of the  
421 biobased polymers followed different patterns regarding the  
422 morphological characteristic of each matrix. As can be seen in  
423 Figure 5a, the biodegradation occurred in both the PHA and  
424 PLA phases.

425 The biodegradation assay revealed that the PHA films  
426 exhibited remarkable biodegradation after 30 days, whereas the  
427 blend matrices (PLA/PHA) showed changes around 50 days,

which indicated a delay in the process of biodegradation 428  
(Figure 5a). According to Weng et al.,<sup>27</sup> a PHA polymer could 429  
be biodegraded at a high rate under composting as well as soil- 430  
environment conditions; in contrast, although PLA was 431  
biodegradable under composting conditions, its degradation 432  
rate in soil was slow. 433

SEM micrographs show the fractured surface of the PLA/ 434  
PHA matrices after a biodegradation process of 50 days 435  
(Figure 5a). It can be seen that the biodegradation was 436  
intensified with higher proportions of PHA in the blend 437  
system. As the proportion of PHA increased, particularly from 438  
40/60 to 20/80, the matrices showed greater interstices or 439  
cavities (Figure 4), which could facilitate the biodegradation 440  
process. Zhang and Thomas<sup>11</sup> explained that the inclusion of 441  
PHA improved the degradation degree of PLA at room 442  
temperature. The authors reported that PHA and PLA exhibit 443  
different degradation patterns. PHA is mainly degraded by the 444  
attack of various enzymes at the surface. According to Weng et 445  
al.<sup>27</sup> the degradation of PHA can be attributed to erosion 446  
catalyzed by bacteria from the surface to the interior. 447

In contrast, PLA degradation is produced throughout the 448  
whole sample, starting with a nonenzymatic hydrolysis that 449  
leads to a reduction in the molecular weight.<sup>11</sup> Then, low- 450  
molecular-weight PLA diffuses out of the bulk polymer and can 451  
be metabolized by microorganisms, producing water, carbon 452  
dioxide, and humus.<sup>29</sup> 453

On the other hand, the thermograms of the 20/80, 40/60 454  
and 60/40 blend matrices exposed to the biodegradation 455  
process for 50 days showed a decrease of the transition 456  
enthalpy, corresponding to the melting of the PHA crystalline 457  
fraction being more marked in the blends with the greatest 458  
proportion of PHA (Figure 5b). In this sense, Dharmalingam<sup>30</sup> 459  
found that the changes of melting enthalpy ( $\Delta H_m$ ) for a 460  
composite material based on PLA/PHA blends represent 461  
depolymerization. Consequently, this phenomenon could 462  
indicate a higher sensitivity to the degradation process in the 463  
presence of higher proportions of PHA, independent of the 464  
rearrangement formed between both polymers. 465

The chemical-structure changes of the matrices exposed to 466  
the biodegradation process were investigated by ATR-FTIR 467  
(Figure 5c). 468

ATR-FTIR spectra corroborated the changes caused in the 469  
structure of the polymers. After 50 days of exposure to the 470  
biodegradation process, ATR-FTIR spectra of the PHA and 471  
blend films showed that the bands lost definition. 472

For all the samples assayed, the peaks in the 4000–3000 473  
cm<sup>-1</sup> region became broadened after the biodegradation 474  
process (data not shown). According to Weng et al.,<sup>27</sup> this 475  
fact was attributable to the formation of hydroxyl and 476  
carboxylic groups. This was also confirmed by the shift of 477  
the absorption peak of the C=O stretching vibration after 478  
biodegradation. 479

Ludueña et al.<sup>31</sup> pointed out that chemical and enzymatic 480  
hydrolysis are the main mechanisms of chain rupture during 481  
the degradation process. Then, biodegradation process 482  
depends on water availability, which produces hydrolysis, and 483  
microbial attack of the matrix. Water diffusion in the soil leads 484  
to a hydrolytic degradation of the material modifying the 485  
surface, resulting in a porous structure with evident signs of 486  
degradation. A similar explanation was proposed by Rocca- 487  
Smith et al.<sup>32</sup> 488

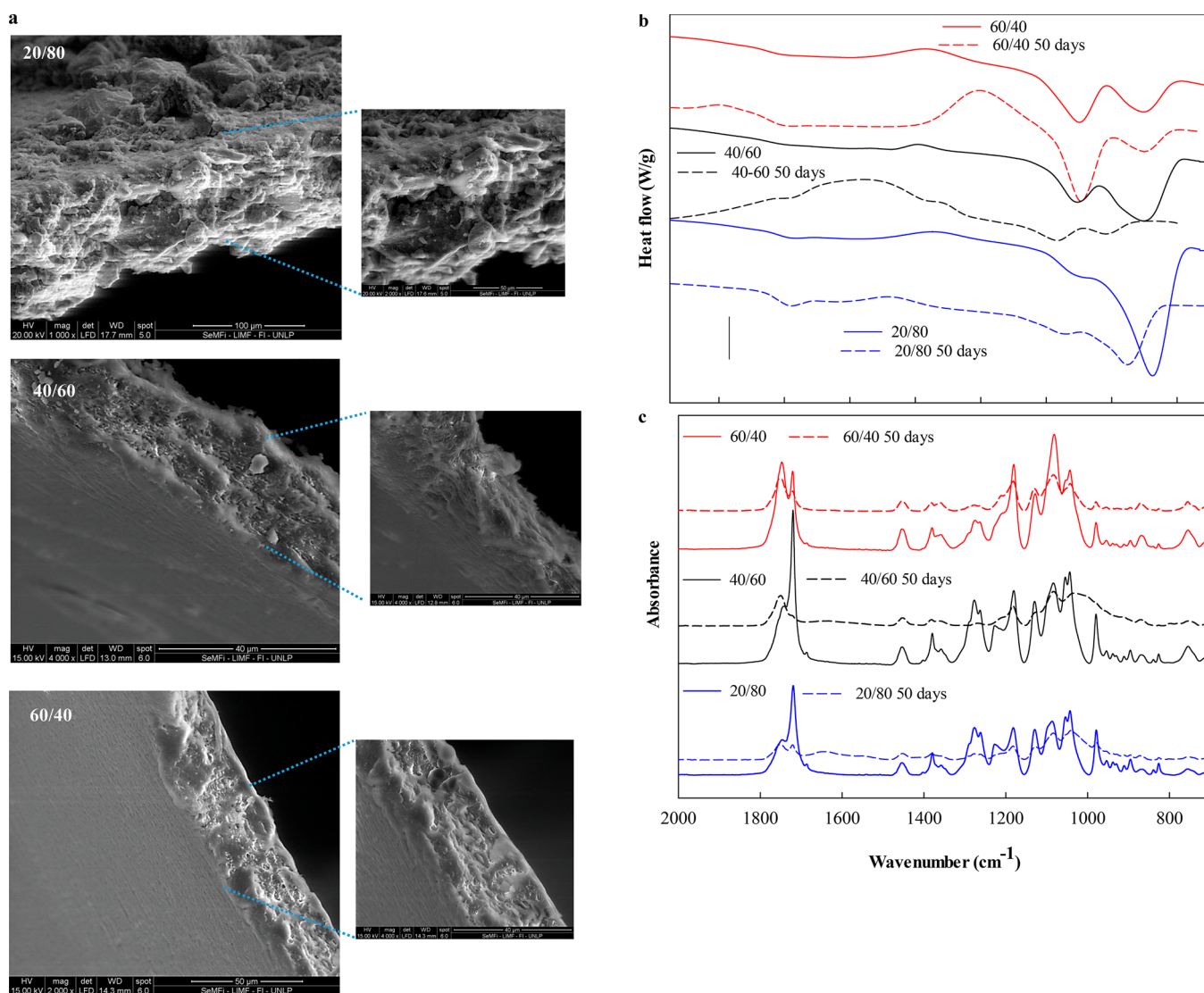


**Figure 5.** Monitoring of the behaviors of samples after they were submitted to biodegradation processes (buried for 50 days) through (a) SEM micrographs of the PLA/PHA blend matrices with enlarged sections showing the degradation (magnification is indicated in the micrographs), (b) MDSC analysis, and (c) FTIR-ATR studies.

489 The biodegradability of the blends was more marked in films  
490 formulated with increasing proportions of PHA; similar results  
491 were reported by Zhang and Thomas.<sup>11</sup>

492 **Conclusions.** Thermal and microstructural studies revealed  
493 that blends of PLA/PHA-based systems were partially miscible.  
494 The formulation of blend matrices improved the crystallinity of  
495 PLA; additionally, it induced the polymer-recrystallization  
496 process, because crystallized PHA acted as a PLA-nucleating  
497 agent. This phenomenon explains the improvements in water-  
498 vapor-barrier film properties. Moreover, the blends exposed to  
499 a biodegradation process showed an intermediate behavior  
500 between those of PLA and PHA, leading to a consistent basis  
501 for designing systems tailored to a particular purpose or use.

502 This work, therefore, contributes to the knowledge of  
503 microstructures, allowing one to develop and test materials  
504 with specific technological applications.

## 505 AUTHOR INFORMATION

### 506 Corresponding Author

507 \*E-mail: [sandra\\_gmr@yahoo.com](mailto:sandra_gmr@yahoo.com). Tel. and Fax: +54 0221-  
508 424-9287, +54 0221-425-4853, or +54 0221-489-0741.

## ORCID

Sandra Rivero: [0000-0002-9002-182X](https://orcid.org/0000-0002-9002-182X)

## Funding

This work was supported by the Argentinean Agency for the  
Scientific and Technological Promotion (ANPCyT; Project  
PICT 2012-0415, 2014-1620), the Argentinean National  
Research Council (CONICET, PIP 2013-0109), and the  
University of La Plata (Argentina).

## Notes

The authors declare no competing financial interest.

## ACKNOWLEDGMENTS

The authors acknowledge Ing. Javier Lecot, Lic. Diana Velasco,  
and Daniel Russo for technical assistance.

## REFERENCES

- (1) Ren, J. *Biodegradable Poly (Lactic Acid): Synthesis, Modification, Processing*; Springer-Verlag: Berlin, 2011.
- (2) Colombo, B.; Sciarria, T. P.; Reis, M.; Scaglia, B.; Adani, F. Polyhydroxyalkanoates (PHAs) production from fermented cheese

- 527 whey by using a mixed microbial culture. *Bioresour. Technol.* **2016**,  
528 *218*, 692–699.
- 529 (3) Mothes, G.; Schnorpfel, C.; Ackermann, J.-U. Production of  
530 PHB from crude glycerol. *Eng. Life Sci.* **2007**, *7*, 475–479.
- 531 (4) Thellen, C.; Coyne, M.; Froio, D.; Auerbach, M.; Wirsén, C.;  
532 Ratto, J. A. A processing, characterization and marine biodegradation  
533 study of melt-extruded polyhydroxyalkanoate (PHA) films. *J. Polym.*  
534 *Environ.* **2008**, *16* (1), 1–11.
- 535 (5) Rivero, S.; Lecot, J.; Pinotti, A. Impregnation of kraft paper  
536 support with polylactic acid multilayers. *Adv. Mater. Lett.* **2017**, *8* (6),  
537 741–751.
- 538 (6) Madhavan Nampoothiri, K.; Nair, N. R.; John, R. P. An overview  
539 of the recent developments in polylactide (PLA) research. *Bioresour.*  
540 *Technol.* **2010**, *101* (22), 8493–8501.
- 541 (7) Sin, L. T. *Polylactic Acid: PLA Biopolymer Technology and*  
542 *Applications*, 1st ed.; Elsevier, 2012.
- 543 (8) Murariu, M.; Dubois, P. PLA composites: From production to  
544 properties. *Adv. Drug Delivery Rev.* **2016**, *107*, 17–46.
- 545 (9) Armentano, I.; Fortunati, E.; Burgos, N.; Dominici, F.; Luzi, F.;  
546 Fiori, S.; Jiménez, A.; Yoon, K.; Ahn, J.; Kang, S.; Kenny, J. M.  
547 Processing and characterization of plasticized PLA/PHB blends for  
548 biodegradable multiphase systems. *eXPRESS Polym. Lett.* **2015**, *9* (7),  
549 583–596.
- 550 (10) Abdelwahab, M. A.; Flynn, A.; Chiou, B. S.; Imam, S.; Orts, W.;  
551 Chiellini, E. Thermal, mechanical and morphological characterization  
552 of plasticized PLA–PHB blends. *Polym. Degrad. Stab.* **2012**, *97* (9),  
553 1822–1828.
- 554 (11) Zhang, M.; Thomas, N. L. Blending polylactic acid with  
555 polyhydroxybutyrate: the effect on thermal, mechanical, and  
556 biodegradation properties. *Adv. Polym. Technol.* **2011**, *30* (2), 67–79.
- 557 (12) Arrieta, M. P.; López, J.; Hernández, A.; Rayón, E. Ternary  
558 PLA–PHB–Limonene blends intended for biodegradable food  
559 packaging applications. *Eur. Polym. J.* **2014**, *50*, 255–270.
- 560 (13) Arrieta, M. P.; Castro-Lopez, M. D. M.; Rayón, E.; Barral-  
561 Losada, L. F.; López-Vilariño, J. M.; López, J.; González-Rodríguez,  
562 M. V. Plasticized poly (lactic acid)–poly (hydroxybutyrate)(PLA–  
563 PHB) blends incorporated with catechin intended for active food-  
564 packaging applications. *J. Agric. Food Chem.* **2014**, *62* (41), 10170–  
565 10180.
- 566 (14) Arrieta, M. P.; Fortunati, E.; Dominici, F.; López, J.; Kenny, J.  
567 M. Bionanocomposite films based on plasticized PLA–PHB/cellulose  
568 nanocrystal blends. *Carbohydr. Polym.* **2015**, *121*, 265–275.
- 569 (15) Venkateswar Reddy, M.; Nikhil, G. N.; Venkata Mohan, S.;  
570 Swamy, Y. V.; Sarma, P. N. *Pseudomonas otitidis* as a potential  
571 biocatalyst for polyhydroxyalkanoates (PHA) synthesis using  
572 synthetic wastewater and acidogenic effluents. *Bioresour. Technol.*  
573 **2012**, *123*, 471–479.
- 574 (16) Rivero, S.; García, M. A.; Pinotti, A. Crosslinking capacity of  
575 tannic acid in plasticized chitosan films. *Carbohydr. Polym.* **2010**, *82*  
576 (2), 270–276.
- 577 (17) Standard test methods for water vapor transmission of material.  
578 In *Annual book of ASTM*, E96-95; American Society for Testing and  
579 Materials: Philadelphia, PA, 1995.
- 580 (18) Lamarra, J.; Giannuzzi, L.; Rivero, S.; Pinotti, A. Assembly of  
581 chitosan support matrix with gallic acid-functionalized nanoparticles.  
582 *Mater. Sci. Eng., C* **2017**, *79*, 848–859.
- 583 (19) Villarruel, S.; Giannuzzi, L.; Rivero, S.; Pinotti, A. Changes  
584 induced by UV radiation in the presence of sodium benzoate in films  
585 formulated with polyvinyl alcohol and carboxymethyl cellulose. *Mater.*  
586 *Sci. Eng., C* **2015**, *56*, 545–554.
- 587 (20) Rivero, S.; García, M. A.; Pinotti, A. Physical and chemical  
588 treatments on chitosan matrix to modify film properties and kinetics  
589 of biodegradation. *J. Mater. Physics Chem.* **2013**, *1* (3), 51–57.
- 590 (21) Standard Test Method for determining aerobic biodegradation  
591 in soil of plastic materials or residual plastic materials after  
592 composting. In *Annual book of ASTM*, D5988-03; American Society  
593 for Testing and Materials: Philadelphia, PA, 2003.
- 594 (22) da Silva, M. G. D.; Vargas, H.; Poley, L. H.; Rodriguez, R. S.;  
595 Baptista, G. B. Structural impact of hydroxyvalerate in polyhydrox-  
yalkanoates (PHAs) dense film monitored by XPS and photo-  
thermal methods. *J. Braz. Chem. Soc.* **2005**, *16* (4), 790–795.
- (23) Ikehara, T.; Kimura, H.; Qiu, Z. Penetrating spherulitic growth  
in poly (butylene adipate-co-butylene succinate)/poly (ethylene  
oxide) blends. *Macromolecules* **2005**, *38* (12), 5104–5108.
- (24) Lipatov, Y. S.; Alekseeva, T. *Phase-Separated Interpenetrating*  
*Polymer Networks*; Springer-Verlag: Berlin, 2007.
- (25) Furukawa, T.; Sato, H.; Murakami, R.; Zhang, J.; Duan, Y. X.;  
Noda, I.; Ochiai, S.; Ozaki, Y. Structure, dispersibility, and crystallinity  
of poly (hydroxybutyrate)/poly (L-lactic acid) blends studied by FT-  
IR microspectroscopy and differential scanning calorimetry. *Macro-*  
*molecules* **2005**, *38* (15), 6445–6454.
- (26) Ashok, B.; Naresh, S.; Reddy, K. O.; Madhukar, K.; Cai, J.;  
Zhang, L.; Rajulu, A. V. Tensile and Thermal Properties of Poly(lactic  
acid)/Eggshell Powder Composite Films. *Int. J. Polym. Anal. Charact.*  
**2014**, *19*, 245–255.
- (27) Weng, Y. X.; Wang, L.; Zhang, M.; Wang, X. L.; Wang, Y. Z.  
Biodegradation behavior of P (3HB, 4HB)/PLA blends in real soil  
environments. *Polym. Test.* **2013**, *32* (1), 60–70.
- (28) Reis, M. O.; Olivato, J. B.; Bilck, A. P.; Zanela, J.; Grossmann,  
M. V. E.; Yamashita, F. Biodegradable trays of thermoplastic starch/  
poly (lactic acid) coated with beeswax. *Ind. Crops Prod.* **2018**, *112*,  
481–487.
- (29) Auras, R.; Harte, B.; Selke, S. An Overview of polylactides as  
packaging materials. *Macromol. Biosci.* **2004**, *4*, 835–864.
- (30) Dharmalingam, S. *Biodegradation and photodegradation of*  
*polylactic acid and polylactic acid/polyhydroxyalkanoate blends non-*  
*woven agricultural mulches in ambient soil conditions*. Ph.D.  
Dissertation, University of Tennessee, Knoxville, TN, 2014.
- (31) Ludueña, L.; Vázquez, A.; Alvarez, V. Effect of lignocellulosic  
filler type and content on the behavior of polycaprolactone based eco-  
composites for packaging applications. *Carbohydr. Polym.* **2012**, *87*,  
411–421.
- (32) Rocca-Smith, J. R.; Chau, N.; Champion, D.; Brachais, C. H.;  
Marcuzzo, E.; Sensidoni, A.; Piasente, F.; Karbowiak, T.; Debeaufort,  
F. Effect of the state of water and relative humidity on ageing of PLA  
films. *Food Chem.* **2017**, *236*, 109–119.